Journal of Low Temperature Physics (2025) 219:79–86
https://doi.org/10.1007/s10909-025-03277-4

MISTRAL: Science Perspectives and Performance Forecasts

G. Isopi[1] · E. Barbavara[1] · E. S. Battistelli[1,2] · P. de Bernardis[1,2] · F. Cacciotti[1] · V. Capalbo[1] · A. Carbone[1] · E. Carretti[3] · D. Ciccalotti[1] · F. Columbro[1,2] · A. Coppolecchia[1,2] · A. Cruciani[2] · G. D' Alessandro[1,2] · M. De Petris[1,2] · F. Govoni[4] · L. Lamagna[1,2] · E. Levati[1] · P. Marongiu[4] · A. Mascia[4] · S. Masi[1,2] · E. Molinari[7] · M. Murgia[4] · A. Navarrini[4] · A. Novelli[1] · A. Occhiuzzi[1] · A. Orlati[3] · A. Paiella[1,2] · E. Pappalardo[1] · G. Pettinari[5] · F. Piacentini[1,2] · T. Pisanu[4] · S. Poppi[4] · I. Porceddu[4] · A. Ritacco[4,6] · M. R. Schirru[4] · G. Vargiu[4]

Received: 2 November 2023 / Accepted: 13 February 2025 / Published online: 7 April 2025

Abstract
The MIllimeter Sardinia radio Telescope Receiver based on Array of Lumped elements (MISTRAL) KIDs is a millimeter camera operating at 90GHz that was recently installed on the Sardinia Radio Telescope (SRT) as part of the SRT-High-Freq program, which aims to expand the capabilities of the radio telescope up to the W-band. After technical and scientific commissioning (2023–2024), MISTRAL will be open to proposals from scientists as a facility instrument. MISTRAL provides a wide 4' field of view, sampled at a resolution of 12" with approximately 400 kinetic inductance detectors. The sky in the W-band is well explored by CMB experiments; however, their resolution is limited to about 1'. Using large single-dish radio telescopes like SRT or the Green Bank Telescope allows to probe angular scales down to 10–12", allowing scientists to obtain new data and complementary information in multiple scientific cases. In this contribution, we will review observational perspectives and performance forecasts of MISTRAL, based on laboratory measurements of the noise properties, for selected scientific cases such as galactic science and high-resolution measurements of the Sunyaev–Zel'Dovich effect in galaxy clusters and in the cosmic web.

Keywords MISTRAL · High angular resolution · Sunyaev–Zel'Dovich effect · Forecast

Extended author information available on the last page of the article

Table 1 State-of-the-art instruments

Instrument	Frequency [GHz]	resolution ["]	FOV [']
MUSTANG-2	90	9	4
MISTRAL	90	12.2	4
NIKA2	150/260	11/18	6.5
TolTEC	150/220/270	9.5/6.3/5	4
Nobeyama 100 GHz	100	16.7	3

1 MISTRAL in a Nutshell

MISTRAL is a total power millimeter camera operating at 90GHz, installed at the Gregorian focus of the Sardinia Radio Telescope (SRT). Coupled to the 64m antenna, 60 m of which are illuminated to prevent spillover and obtain diffraction-limited performance, it will provide a resolution of 12.2" on the optical axis. MISTRAL is part of the SRT-HighFreq project, funded by a Programma Organizzativo Nazionale (PON), aimed to expand the capabilities of SRT up to the W-band. After technical and scientific commissioning, MISTRAL will be open to proposals from the scientific community as a facility instruments. The instrument is enclosed in a custom, four-stage cryostat provided by QMC[1] that contains the re-imaging optics and cools down to $\sim 200 - 240mK$ [1], the array of 415 kinetic inductance detectors (KIDs) [2–5]. The array covers a diffraction-limited, almost Nyquist-sampled ($0.7\ f\lambda$) field of view of 4'. The pulse tube head is fixed to the cryostat and the valve is fixed to the structural frame, while the compressor is located at the base of the telescope, connected with 100 m of flexible helium lines [6]. The sub-K refrigerator and the pulse tube cryocooler are tilted by 57.5° with respect to the focal plane in order to obtain the maximum cooling efficiency when the telescope is tilted at elevations between 32.5° and 82.5°. This allows MISTRAL to observe the northern sky down to a declination of −7°, giving access to ∼ 60% of the sky, with great overlap to other state of the art instruments.

1.1 MISTRAL in the International Framework

Currently, only few cameras able to observe in the millimeter regime at high resolution (N10") exist in the world. Notable examples are MUSTANG-2 at the Green Bank Telescope (GBT), NIKA2 at IRAM, TolTEC at the Large Millimeter Telescope (LMT) and the 100GHz MKID Camera at Nobeyama-45 m (see Table 1). The addition of a new receiver in the same band will provide a new stream of data to the millimeter science community, with high complementarity with the receivers operating at different frequencies with similar resolution. Millimeter cameras also offer great synergy with CMB survey telescopes and interferometers. CMB telescopes are characterized by a relatively low resolution ($\approx 1'$ from the ground, $\approx 10'$ from

[1] http://www.qmcinstruments.co.uk/

space) and a large field of view (FOV) which provides a high mapping speed. On the other hand, interferometers like ALMA provide a sub-arcsecond resolution but cannot recover angular scales larger than $\approx 1'$ (42" at 100GHz using ALMA Compact Array[2]). Millimeter cameras fill the gap between interferometers and CMB telescopes, enabling full characterization of sources without losing information at intermediate scales.

2 Science Cases

2.1 High-Resolution tSZe

The thermal Sunyaev–Zel'Dovich effect (tSZe) is an anisotropic spectral distortion of the cosmic microwave background (CMB) caused by the inverse Compton scattering between the cold CMB photons and a population of hot electrons like in the intra-cluster medium (ICM) of galaxy clusters. This scattering process results in a net transfer of energy from electrons to photons that are upscattered from low frequencies to higher frequencies. This causes a decrement of brightness at low frequencies, which means that clusters will cast "shadows" on the CMB.

The tSZe spectral distortion can be written as:

$$\frac{\Delta I(x)}{I_0} = y\frac{x^4 e^x}{(e^x-1)^2}\left(x\coth\frac{x}{2}-4\right) := yg(x)$$

where $x = h\nu/\left(k_b T_{CMB}\right)$ is the adimensional frequency and y is the Comptonization parameter, which is proportional to the product between electron density n_e and electron temperature T_e integrated along the line of sight (LOS):

$$y = \frac{\sigma_T}{m_e c^2}\int_{\mathrm{LOS}} n_e(r) k_B T_e(r)\,\mathrm{d}r$$

Since tSZe traces the electron pressure, one can take advantage of millimeter observations to better understand the physics of galaxy clusters, which are very interesting astrophysical environments, being the largest collapsed structures in the universe, half-way between galactic and cosmological scales. High-resolution observations can be used to characterize pressure profiles and small-scale structures like pressure fluctuations and shocks, in order to infer the dynamical state and the past history of interactions and mergers between clusters, as well as better calibrating the $Y{-}M$ relation, where Y is the integrated Compton-y parameter and M is the mass of the cluster.

Additionally, since tSZe is visible at low gas temperature and densities, being linear in n_e, it can be used to detect the warm-hot intergalactic medium (WHIM) expected to trace the cosmic web, a network of filamentary structures connecting galaxy clusters, in which we expect to find almost half of the baryonic matter of the

[2] https://almascience.eso.org/proposing/cycle2-call-for-proposals/capabilities.

universe. These filaments are predicted by cosmological simulations, yet very difficult to observe. An interesting case study for the cosmic web is the Abell 401–Abell 399 cluster system, where a high significance detection of a bridge connecting the two clusters has been obtained using data from the Atacama Cosmology Telescope (ACT) and the MUSTANG-2 receiver [7]. High-resolution observations gave evidence that the clusters did not interact in the past; therefore, the bridge between them is a cosmological filament being compressed and heated as the clusters gravitate toward each other. MISTRAL will provide additional observational capacity to characterize the small-scale structures in this particular system and other relevant multiple systems in the sky.

2.2 Galactic and Extragalactic Science

Many astrophysical processes occur in the W-band. This frequency is located at the minimum between thermal emission of the dust and synchrotron/free-free emission. This band is thus important to disentangle different emission processes in galactic and extragalactic environments, especially if coupled with the observations of other high-resolution receivers in the millimeter domain. Observing our galaxy at high resolution will help to characterize small features like dense cores in star forming regions, protoplanetary disks or compact nebulae, currently unresolved by CMB experiments. The large field of view and mapping speed will enable wide area continuum surveys for blind detection of these sources. Additionally, this high resolution allows to resolve nearby galaxies and provide spatially resolved understanding of the radiative processes happening outside the Milky Way [8]. Another interesting case study accessible with MISTRAL is the characterization of compact sources in the millimeter domain. These sources are not resolved by CMB experiments, but could result in a bias if not modeled correctly, especially in cluster cosmology where cluster parameters (like the integrated Compton-y parameter) can be contaminated by point sources [9].

3 Sensitivity Forecast

The main source of noise for MISTRAL will be the atmospheric emission, which is in turn very sensitive on the water vapor content of the atmosphere. For this reason, the sensitivity will be highly dependent on the weather, the elevation of the object, the scanning strategy and the map-making pipeline. As a preliminary estimate, we computed the on-sky sensitivity of MISTRAL from the noise time-streams acquired during the laboratory calibration phase, illuminating the focal plane with a slab of Eccosorb at an ambient temperature of ≈ 300K. We considered this radiative background as a pessimistic case, as we expect a lower brightness temperature when observing from SRT site in the W-band.

We considered the noise equivalent power (NEP) of the detectors at a frequency of 10 Hz, expected to be the frequency at which astrophysical signals will be modulated, given the scanning speed and strategy. At 10 Hz, we measured an

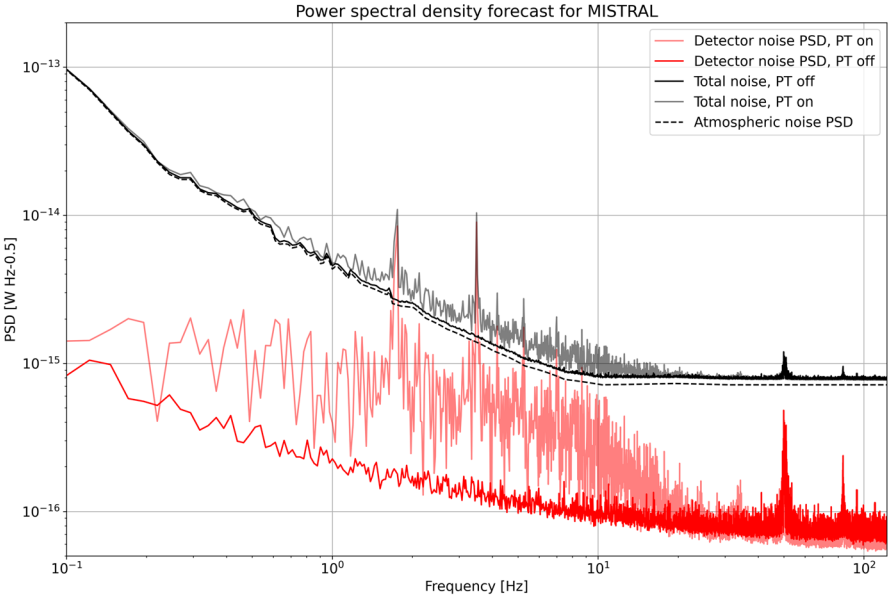

Fig. 1 Measured average PSD of the detectors compared to an atmospheric model at an elevation of 45° generated using the `maria` python package. At high frequency, the photon noise from the atmosphere dominates. At lower frequency, the noise is dominated by slow atmosphere fluctuations. We observe an excess of noise up to 10Hz caused by residual vibrations from the cryocooler, which will be suppressed after the installation of MISTRAL on its final support at SRT

array-averaged $NEP = 8 \times 10^{-16} WHz^{-0.5}$ (Fig. 1) at the window of MISTRAL. The NEP is calculated by dividing the phase noise by the measured array-averaged optical responsivity, which is $3 \times 10^{11} rad/W$ [3, 4]. We used this value to compute the Noise Equivalent Flux Density (NEFD) [10] in 1s of integration, assuming a telescope efficiency $\eta = 0.3$ (expected efficiency for an antenna with a surface RMS of $250\mu m$):

$$\mathrm{NEFD} = \frac{\mathrm{NEP}}{\sqrt{2} A_{\mathrm{SRT}} \Delta\nu \eta} = 2.8 mJy\sqrt{s}$$

where A_{SRT} is the area of the main dish of SRT, stopped at 60m and $\Delta\nu = 26$GHz is the bandwidth of MISTRAL. This NEFD assumes that the map-making pipeline efficiently filters the low frequency atmospheric noise, which is a reasonable assumption for point or compact sources, as their power is modulated at high frequencies. In our case, we removed the common mode, averaged along all the pixels. We repeated this estimate for a case in which we want to recover larger angular scales (> 4') by applying a less aggressive filter. Since MISTRAL will be the first receiver to observe in the W-band from SRT, we estimated the expected atmospheric fluctuations starting from archival data in the K-band. These fluctuations in average conditions (50th percentile) were found to be $5mJy\sqrt{s}$, independently from the applied filters to the time-streams: a second-order polynomial and high-pass filters at

0.5 and 1 Hz. We then rescaled this value according to the different opacity expected in the W-band for the SRT site [11]:

$$\sigma_{W,50\text{th}} = \sigma_{K,50\text{th}} \left(\frac{\tau_{K,50\text{th}}}{\tau_{W,50\text{th}}} \right)^2 \implies \sigma_{W,i-\text{th}} = \sigma_{W,50\text{th}} \left(\frac{\sigma_{W,i-\text{th}}}{\sigma_{W,50\text{th}}} \right)^2$$

where σ_K and σ_W are the atmospheric fluctuation RMS for K- and W-band, $\tau_{K,i-\text{th}}$ and $\tau_{W,i-\text{th}}$ are the atmospheric opacities for the K- and W-band in the $i-$th percentile. Following the former equation, we obtain NEFD $= 5 - 15 mJy\sqrt{\text{s}}$, considering the 5th and 95th percentile of precipitable water vapor (PWV). We used this NEFD value to compute the predicted mapping speed [10]:

$$M_S = \eta \frac{\pi}{4} d_{\text{FOV}}^2 \frac{1}{\text{NEFD}^2} = (170 - 1500)\ \text{arcmin}^2/mJy^2/h$$

which is comparable to the other state of the art instruments. Given the high variability of the atmospheric conditions, MISTRAL observations will be scheduled in the best conditions according to the needed sensitivity (dynamic scheduling). Deep observations of faint, extended sources like galaxy clusters will be scheduled in the best possible conditions, while observations of compact, bright sources will be possible in less than optimal conditions. We further tested the sensitivity predictions by injecting sources into the noise time-streams acquired during laboratory calibrations. We used the measured IQ loops to convert the power received by a KID from a simulated astrophysical source to raw I and Q time-streams readout by the ROACH2 FPGA, then converted them in a normalized phase time-stream, added the atmospheric noise model shown in Fig. 1 and wrote it on a FITS file. We then reconstructed a map of a simulated scan (Fig. 2) and measured the residual noise in the map before and after filtering. By filtering the raw time-streams with removing a common mode from all the pixels, we obtain a residual noise of $\sigma_{\text{map}} \approx 5 mJy$, consistent with the previous estimates.

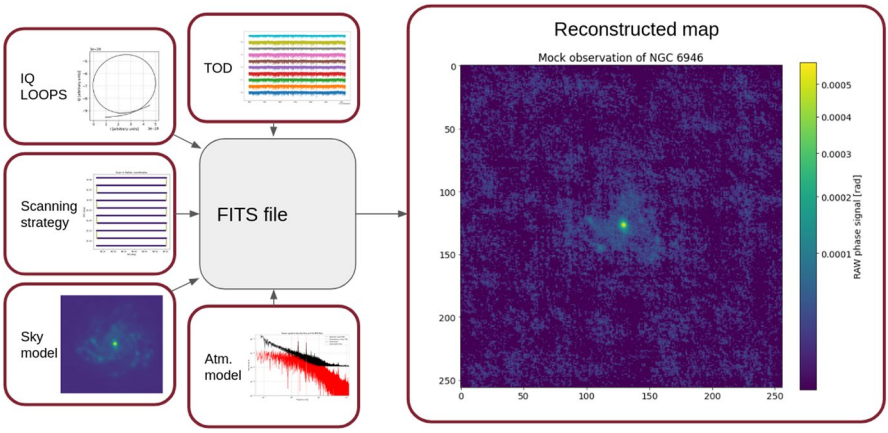

Fig. 2 Outline of the simulation framework. In this example we reconstructed the map of an NGC6946-like spiral galaxy

4 Conclusion

ISTRAL is a new millimeter camera recently installed at the Sardinia Radio Telescope and will observe the 90 GHz sky with a field of view of 4' and a resolution of 12″. We used noise time-streams acquired during the laboratory calibration phase to produce a forecast of the performance of the receiver on the sky, estimating a NEFD between 5 and 15 mJy for 1s of integration, depending on atmospheric conditions. Additionally, we injected into the noise time-streams different sky models and an atmospheric noise model to estimate the residual noise of the reconstructed map after the map-making pipeline and found results consistent with the NEFD estimate presented before. This sensitivity forecast is highly sensitive on the atmospheric conditions and will be refined in the technical and scientific commissioning phase of the receiver, expected for late 2023–2024. If we integrate the tSZ spectrum along the MISTRAL band, we can derive a Compton-y sensitivity for the best case mapping speed, which is $\sigma_y = 4 \times 10^{-5}$ when scanning a 1arcmin^2 region for one hour. Assuming the cluster parameters observed in [12], we conclude that MISTRAL will be able to observe Abell 399 and Abell 401 with a signal to noise ratio of, respectively, 2 and 3. The wide field of view and high mapping speed of MISTRAL will also allow wide area continuum surveys of our galaxy, with great complementarity with interferometers, and with CMB survey instruments. After commissioning, MISTRAL will be open to proposals as a facility instruments and will be a key instrument for high resolution, wide area surveys in the W-band. Observations of this kind will provide precious data from a plethora of science cases, spanning from the physics of galaxy clusters and the cosmic web, to the properties of interstellar dust and observation of galactic and extragalactic sources.

Funding Open access funding provided by Università degli Studi di Roma La Sapienza within the CRUI-CARE Agreement.

References

1. A. Coppolecchia et al., Cryogenic performance of the MISTRAL instrument. J. Low Temp. Physi. This Special Issue (2023)
2. A. Coppolecchia et al., W-band lumped element kinetic inductance detector array for large ground-based telescopes. J. Low Temp. Phys. (2020). https://doi.org/10.1007/s10909-019-02275-7
3. A. Paiella et al., MISTRAL and its KIDs. J. Low Temp. Phys. **209**, 889–898 (2022). https://doi.org/10.1007/s10909-022-02848-z
4. A. Paiella et al., The MISTRAL instrument and the characterization of its focal plane. J. Low Temp. Phys. This Special Issue (2023)

5. F. Cacciotti et al., Dark performance of the MISTRAL LEKIDs. J. Low Temp. Phys. This Special Issue (2023)
6. A. Coppolecchia et al., Pulse tube cooler with > 100 m flexible lines for operation of cryogenic detector arrays at large radiotelescopes. J. Low Temp. Phys. **211**, 415–425 (2023). https://doi.org/10.1007/s10909-022-02934-2
7. A.D. Hincks et al., A high-resolution view of the filament of gas between Abell 399 and Abell 401 from the Atacama Cosmology Telescope and MUSTANG-2. Monthly Notices of the Royal Astronomical Society **510**(3), 3335–3355 (2021). https://doi.org/10.1093/mnras/stab3391 https://academic.oup.com/mnras/article-pdf/510/3/3335/42147540/stab3391.pdf
8. G. Ejlali et al., Dust Emission in Galaxies at Millimeter Wavelengths: Cooling of Star Forming Regions in NGC6946, vol. **257** (2022). https://doi.org/10.1051/epjconf/20222570001
9. S. Dicker et al., Observations of compact sources in galaxy clusters using MUSTANG2. In: Monthly Notices of the Royal Astronomical Society 508 (2021). https://doi.org/10.1093/mnras/stab267
10. L. Perotto et al., Calibration and performance of the nika2 camera at the iram 30-m telescope. Astron. Astrophys. **637** (2020). https://doi.org/10.1051/0004-6361/201936220
11. J. Sayers, S.R. Golwala, P.A.R. Ade, J.E. Aguirre, J.J. Bock, S.F. Edgington, J. Glenn, A. Goldin, D. Haig, A.E. Lange, G.T. Laurent, P.D. Mauskopf, H.T. Nguyen, P. Rossinot, J. Schlaerth, Studies of millimeter-wave atmospheric noise above mauna kea. Astrophys. J. **708**(2), 1674–1691 (2010). https://doi.org/10.1088/0004-637X/708/2/1674. arXiv:0904.3943 [astro-ph.IM]
12. A. Hincks et al., A high-resolution view of the filament of gas between Abell 399 and Abell 401 from the Atacama Cosmology Telescope and MUSTANG-2. In: Monthly Notices of the Royal Astronomical Society

Authors and Affiliations

G. Isopi[1] · E. Barbavara[1] · E. S. Battistelli[1,2] · P. de Bernardis[1,2] · F. Cacciotti[1] · V. Capalbo[1] · A. Carbone[1] · E. Carretti[3] · D. Ciccalotti[1] · F. Columbro[1,2] · A. Coppolecchia[1,2] · A. Cruciani[2] · G. D' Alessandro[1,2] · M. De Petris[1,2] · F. Govoni[4] · L. Lamagna[1,2] · E. Levati[1] · P. Marongiu[4] · A. Mascia[4] · S. Masi[1,2] · E. Molinari[7] · M. Murgia[4] · A. Navarrini[4] · A. Novelli[1] · A. Occhiuzzi[1] · A. Orlati[3] · A. Paiella[1,2] · E. Pappalardo[1] · G. Pettinari[5] · F. Piacentini[1,2] · T. Pisanu[4] · S. Poppi[4] · I. Porceddu[4] · A. Ritacco[4,6] · M. R. Schirru[4] · G. Vargiu[4]

✉ G. Isopi
giovanni.isopi@roma1.infn.it

[1] Department of Physics, Sapienza University of Rome, Rome, Italy

[2] Istituto Nazionale di Fisica Nucleare, Sezione di Roma 1, Rome, Italy

[3] Istituto di Radioastronomia, Istituto Nazionale di Astrofisica, Bologna, Italy

[4] Osservatorio Astronomico di Cagliari, Istituto Nazionale di Astrofisica, Cagliari, Italy

[5] Istituto di Fotonica e Nanotecnologie, Consiglio Nazionale delle Ricerche, Roma, Italy

[6] LPENS, ENS, PSL Research Univ., CNRS, Sorbonne Univ., Université de Paris, 75005 Paris, France

[7] Osservatorio Astronomico di Brera e REM, Istituto Nazionale di Astrofisica, Milan, Italy